Materials Letters 287 (2021) 129240

Contents lists available at ScienceDirect

Materials Letters

journal homepage: www.elsevier.com/locate/mlblue

The effects of impurities on the generalized stacking fault energy of InP by first-principles calculation

Chengru Wang [a], Han Wu [b], Hong Zhu [a,d,*], Yan-Ting Sun [c], Chaoying Xie [a,*]

[a] School of Materials Science and Engineering, Shanghai Jiao Tong University, Shanghai 200240, China
[b] School of Physical Science and Technology, ShanghaiTech University, Shanghai 201210, China
[c] Department of Applied Physics, School of Engineering Sciences, KTH-Royal Institute of Technology, Roslagstullsbacken 21, 114 21 Stockholm, Sweden
[d] University of Michigan–Shanghai Jiao Tong University Joint Institute, Shanghai Jiao Tong University, Shanghai 200240, China

ARTICLE INFO

Article history:
Received 5 November 2020
Received in revised form 12 December 2020
Accepted 20 December 2020
Available online 24 December 2020

Keywords:
Indium phosphide
Impurity
Stacking faults
First-principles calculations

ABSTRACT

This work investigates the impurity effects on the generalized stacking fault energy (GSFE) of InP via first-principles calculations. The impurity elements of group Ⅳ and VI, which substitute the P sublattice preferentially, are studied here. It is found that the GSFEs of InP will decrease considerably when these impurities are incorporated in the glide plane. The charge density maps indicate that the reduction of GSFEs is predominantly attributed to the electronic effects. These results could contribute to understanding the stacking fault characteristics of III-Ⅴ compounds incorporated by different impurities.

1. Introduction

Possessing outstanding optoelectronic properties, III-Ⅴ compounds have attracted a great deal of attentions for a long time [1]. However, the random stacking faults (SFs) are inevitable in III-Ⅴ compounds, especially when integrated on Si [2]. These random SFs will affect the optoelectronic performance detrimentally [3], while periodic SFs are intriguing for electronic band engineering by introducing miniband [4].

Noteworthily, the impurities probably play considerable role in the generation of SFs according to the observation of massive microtwins in S-doped InP crystals [5] and the controllable preparation of twining superlattices in InP nanowires by Zn doping [6]. This is inspiring, because doping is a route of flexibility to control SFs compared to the precise manipulation of various growth parameters. Furthermore, the generalized stacking fault energy (GSFE) is closely associated with the formation of SFs by the shear deformation or the slip of dislocations [7]. However, as one of the most important III-Ⅴ compounds, the GSFEs of InP incorporated by various impurities are still lacking now.

The method of first-principles calculations have been used widely to study the optical [8], electronic [3,9], magnetic [10], and mechanical [7,11] properties of various materials. To elucidate the mechanism of interactions between impurities and SFs in InP, the GSFEs of InP incorporated by various impurities are investigated by the first-principles calculations in this work.

2. Methods of calculation

The first-principles calculations were implemented in the Vienna ab initio Simulation Package (VASP) software. The $2 \times 2 \times 2$ supercells of InP containing one X atom (X = N, As, Sb, Bi, O, S, Se, Te) were created to identify the preferred substitutional site of X atom by calculating the formation energy: $E_f = E_{total}^{InP-X} - E_{total}^{InP} + E_{element}^{In\ or\ P} - E_{element}^{X}$ [12], where E_{total} is the total energy of supercells, $E_{element}$ represents the energy of In, P, or X atom in their stable elementary state.

To calculate the GSFEs, a slab supercell (see Fig. 1(a)) with lattice orientations of x [$1\bar{1}0$], y[$11\bar{2}$], and z[111] was created, which contained 44 atoms. The slab supercell contains 22 atomic layers along z and a 15 Å vacuum layer. Nine transition structures were established between the perfect structure and the intrinsic stacking fault (ISF) structure by slipping the top half of the slab rigidly relative to the bottom half incrementally along y direction. The GSFE was calculated by optimizing these transition structures independently [13], where the atoms were fixed along the y direction to simulate each slipping displacement. The equation of $\gamma(b) = [E(b)\text{-}E_0]/A$ was used to calculated the GSFEs [11], where A

* Corresponding authors at: School of Materials Science and Engineering, Shanghai Jiao Tong University, Shanghai 200240, China.
E-mail addresses: hong.zhu@sjtu.edu.cn (H. Zhu), cyxie@sjtu.edu.cn (C. Xie).

https://doi.org/10.1016/j.matlet.2020.129240
0167-577X/

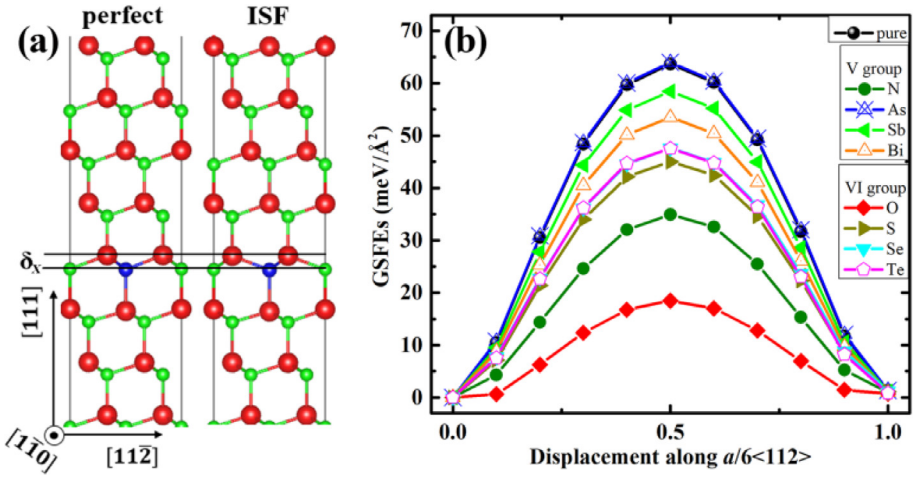

Fig. 1. (a) The structures of perfect, ISF InP. δ_X denotes the average interplanar spacings incorporating *X* atoms. The large (red), medium (blue) and small (green) balls denote the In, *X* and P atoms, respectively. (b) The GSFEs of InP incorporated by various impurities. (For interpretation of the references to colour in this figure legend, the reader is referred to the web version of this article.)

is the glide plane area of supercell, E_0 is the total energy of the perfect supercell, $E(b)$ is the total energy of the relaxed supercell involving *b* displacement of the two rigid slipping parts. The computational details are similar to our previous work [14].

3. Results and discussions

3.1. Site preference of incorporated elements

The formation energies in Table 1 indicate that the energy required for *X* atom to substitute a P atom is smaller than that required to substitute an In atom. This means that the impurity elements concerned here substitute the P atom preferentially in InP.

3.2. GSFEs of impurity incorporated InP

As seen in Fig. 1(a), one P atom on the glide plane was substituted by various impurities. The results in Fig. 1(b) clearly show that the GSFEs of impurity incorporated InP is dramatically reduced relative to that of pure InP, except the As-alloyed InP. For the impurity elements of same period, the GSFEs of VI-doped (n-type doped) InP are smaller than that of Ⅴ-alloyed (isovalent alloyed) InP. This phenomenon could be caused by the introduction of shallow levels in the band gap of n-type InP [15] except the O element that will form deep level. The electrons in these shallow levels are easy to jump into the conduction band, and then enhance the conductivity of semiconductors in practical applications. Therefore, the less localized electrons incorporated into the covalent bonds around the S, Se, Te atoms will weaken the strength of bonds and make the slip along the doped glide planes easy. This is consistent with the measurement that the SF energies of silicon decrease monotonously with the increasing concentration of n-type dopants [16].

Table 1
The formation energies E_f (eV) when *X* atom substitutes In or P atom in InP.

X atom	In site	P site
N	4.931	1.462
As	1.917	0.139
Sb	2.026	0.716
Bi	1.759	1.269
O	3.156	−1.327
S	3.519	0.133
Se	3.045	0.170
Te	3.053	0.722

3.3. Charge density around impurity atoms

Fig. 2 shows the charge density maps of glide plane, respectively for the unstable stacking fault (USF) and stable stacking fault (SSF), which correspond to the maximum and local minimum values along the curves of GSFEs. Apart from the N and O elements, the high charge density are nearly located identifiably between the In and P or impurities, which is the consequence of the characteristic of covalent bonds. Apparently, for impurities of the same period, the charge densities along In-VI bonds are lower than that of the In-Ⅴ bonds, which leads to the reduced GSFEs of InP by the n-type atoms compared to the isovalent atoms. The similar charge density in the Te and Se-doped, the As-alloyed and pure InP results in the comparable GSFEs. Compared to pure InP, the charge density decreases sequentially for As, Sb, Bi, which is consistent with the sequential reduction of electronegativities. This gives rise to the same decreasing trend of GSFEs, as seen in Fig. 1(b).

The GSFEs of N-alloyed and O-doped InP are extremely low (see Fig. 1(b)). This may be due to the wrapped charge density distribution around the N and O atoms, which is different from the situations of other impurities (see Fig. 2). This could be attributed to the large electronegativity of N and O elements, attracting the electrons strongly. The directivity of the covalent bonds is then weakened by the features of charge density distribution around N and O atoms, which reduces the GSFEs remarkably.

3.4. Effect of interplanar spacings

The average interplanar spacings, δ_X of the optimized glide planes (see Fig. 1(a)), increase as the enlargement of impurity atomic size. Here the δ_X of N, As, Sb, Bi alloyed and pure InP at SSF structure, are 0.611 Å, 0.955 Å, 1.211 Å, 1.366 Å, and 0.852 Å, respectively. The GSFEs of pure InP with the glide interplanar spacings of δ_X corresponding to the Ⅴ-alloyed InP were calculated, as seen in Fig. 3. The USF and SSF energies of pure InP will increase when the interplanar spacings of glide planes deviate from the equilibrium δ_{pure}. This is understandable because the strong localized electrons along the covalent bonds will attempt to restore the compression or stretch, consequently increasing the GSFEs. However, compared to the pure InP, the GSFEs of Ⅴ-alloyed and VI-doped InP all decrease (see Fig. 1(b)), though these impurities devi-

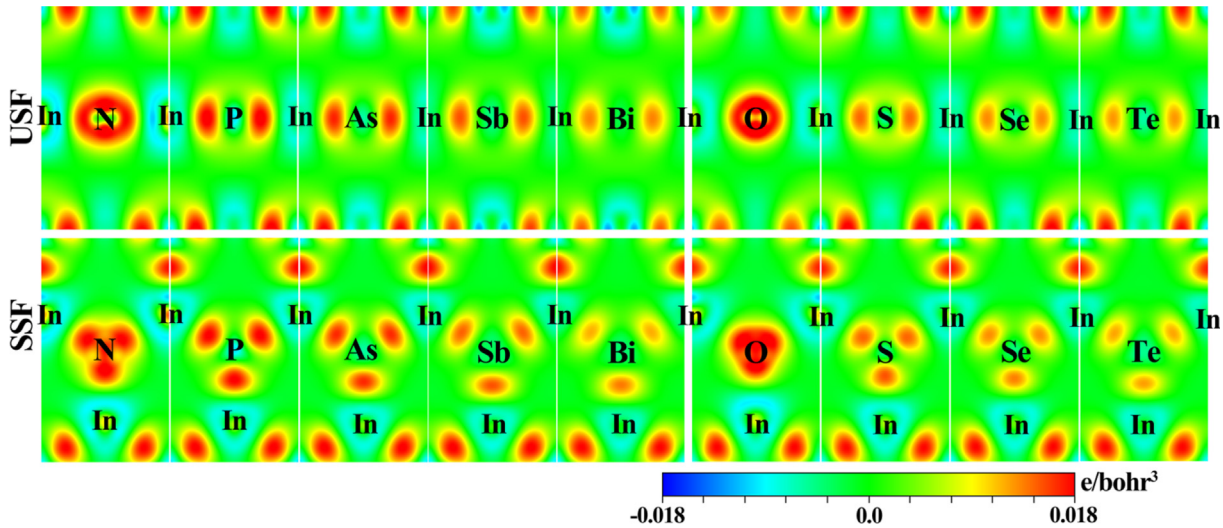

Fig. 2. The charge density maps of glide plane for the USF and SSF structures.

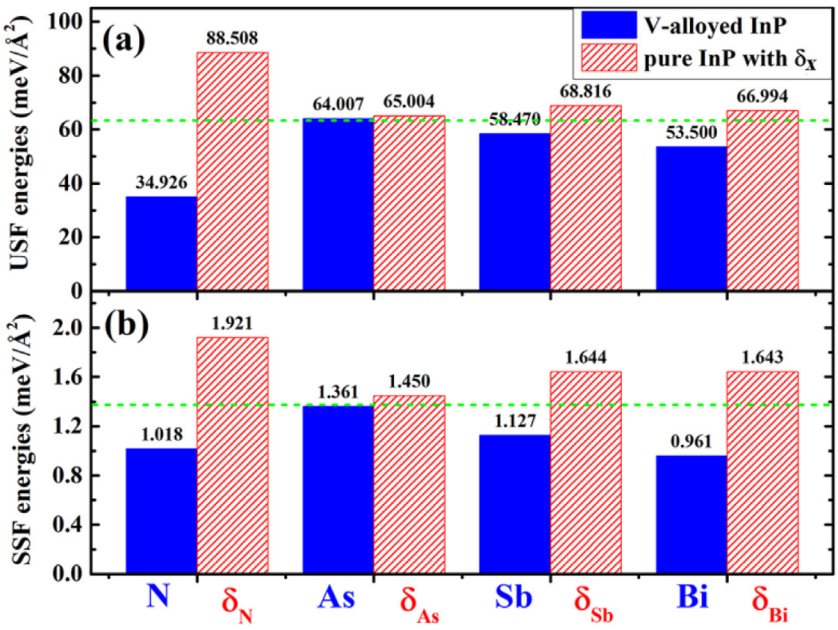

Fig. 3. The USF (a) and SSF (b) energies of Ⅴ-alloyed InP and pure InP with δ_X. The dash lines indicate the results of pure InP with equilibrium δ_{pure}.

ate the interplanar spacings of glide planes from the equilibrium value of pure InP. This further demonstrates that the change of InP GSFEs by doping/alloying these impurities is dominantly attributed to the electronic effects (see Fig. 2), rather than the atomic size of impurities. This is different from the situations of metals. For instance, the GSFEs of copper will decrease as the increase of lattice constants [17]. The reason may be attributed to the characteristics of free electrons in metals that could accommodate to the lattice deformation more easily. There is no denying that more studies are required to explore the impacts of different impurities on the properties of InP and other III-Ⅴ compounds.

4. Conclusions

To summarize, the GSFEs of InP could be reduced significantly by alloying/doping the impurities of Ⅴ/Ⅵ group. For the same period elements, the GSFEs of InP decrease more remarkable by doping the n-type impurities than by alloying the isovalent impurities. Apart from the N element, the GSFEs of Ⅴ-alloyed InP will decrease as the increase of impurity element period. Above GSFE variations of InP incorporated by different impurities are dominantly resulted from the electronic effects between the impurity and the host atoms. Particularly, the valence electrons nearly accumulate around the N and O atoms, which weakens the interplanar bonds. These results could help to understand the characteristics of SFs in InP and other III-Ⅴ compounds.

CRediT authorship contribution statement

Chengru Wang: Conceptualization, Methodology, Investigation, Data curation, Writing - original draft. **Han Wu:** Formal analysis, Visualization. **Hong Zhu:** Resources, Writing - review & editing, Supervision. **Yan-Ting Sun:** Formal analysis, Writing - review & editing. **Chaoying Xie:** Validation, Funding acquisition, Supervision.

Declaration of Competing Interest

The authors declare that they have no known competing financial interests or personal relationships that could have appeared to influence the work reported in this paper.

Acknowledgments

This work was supported by the New-round Discipline Construction of SJTU (2018-2020) Grants: "D & R system for Si-based optoelectronic materials and devices"

References

[1] J.A. del Alamo, Nature 479 (2011) 317–323.
[2] Y.-T. Sun, H. Kataria, W. Metaferia, S. Lourdudoss, CrystEngComm 16 (2014) 7889–7893.
[3] X. Qian, M. Kawai, H. Goto, J. Li, Comp. Mater. Sci. 108 (2015) 258–263.
[4] Z. Ikonic, G.P. Srivastava, J.C. Inkson, Phys. Rev. B 52 (1995) 14078–14085.
[5] M. Azzaz, J.-P. Michel, A. George, Philos. Mag. A 73 (1996) 601–624.
[6] R.E. Algra, M.A. Verheijen, M.T. Borgström, L.-F. Feiner, G. Immink, W.J.P. van Enckevort, E. Vlieg, E.P.A.M. Bakkers, Nature 456 (2008) 369–372.
[7] B.C. De Cooman, Y. Estrin, S.K. Kim, Acta Mater. 142 (2018) 283–362.
[8] Z. Zarhri, M.Á. Avilés Cardos, Y. Ziat, M. Hammi, O. El Rhazouani, J.C. Cruz Argüello, D. Avellaneda Avellaneda, J. Alloys Compd., 819 (2020) 153010.
[9] Y. Ziat, Z. Zarhri, M. Hammi, C. Laghlimi, A. Moutcine, Comp. Condens. Matter 25 (2020) e00502.
[10] Z. Zarhri, M. Houmad, Y. Ziat, O. El Rhazouani, A. Slassi, A. Benyoussef, A. El Kenz, J. Magn. Magn. Mater. 406 (2016) 212–216.
[11] P. Tu, Y. Zheng, C. Zhuang, X. Zeng, H. Zhu, Compos. Mater. Sci. 159 (2019) 357–364.
[12] Q. Dong, Z. Luo, H. Zhu, L. Wang, T. Ying, Z. Jin, D. Li, W. Ding, X. Zeng, J. Mater. Sci. Technol. 34 (2018) 1773–1780.
[13] Y. Su, S. Xu, I.J. Beyerlein, J. Appl. Phys. 126 (2019) 105112.
[14] C. Wang, H. Wu, H. Zhu, C. Xie, Electron. Mater. Lett. 16 (2020) 506–511.
[15] H. Yoshinaga, T. Matsumori, F. Uehara, Jpn. J. Appl. Phys. 35 (1996) 2930–2933.
[16] Y. Ohno, T. Taishi, Y. Tokumoto, I. Yonenaga, J. Appl. Phys. 108 (2010) 073514.
[17] R. Schweinfest, A.T. Paxton, M.W. Finnis, Nature 432 (2004) 1008–1011.